A reified network model for adaptive decision making based on the disconnect-reconnect adaptation principle

Treur, Jan

published in
Network-Oriented Modeling for Adaptive Networks: Designing Higher-Order Adaptive Biological, Mental and Social Network Models

2020

DOI (link to publisher)
10.1007/978-3-030-31445-3_5

document version
Publisher's PDF, also known as Version of record

Chapter 5
A Reified Network Model for Adaptive Decision Making Based on the Disconnect-Reconnect Adaptation Principle

Abstract In recent literature from Neuroscience, the adaptive role of the effects of stress on decision making is highlighted. In this chapter, it is addressed how that role can be modelled computationally using a reified adaptive temporal-causal network architecture. The presented network model addresses the so-called disconnect-reconnect adaptation principle. In the first phase of the acute stress suppression of the existing network connections takes place (disconnect), and then in a second phase after some time there is a relaxation of the suppression. This gives room to quickly get rid of old habits that are not applicable anymore in the new stressful situation and start new learning (reconnect) of better decision making, more adapted to this new stress-triggering context.

Keywords Network reification · Adaptive temporal-causal network model · Hebbian learning · Stress · Decision making

5.1 Introduction

Stress has a strong impact on both cognitive and affective processes. This impact can be experienced as disturbing, but recent findings suggest that its main goal is to improve coping with challenging situations. Stress has bad health effects, as it may cause disorders like depression, anxiety or schizophrenia. But from the positive side, it supports individuals to respond to specific types of threats more adequately, keeping an individual's homeostasis up to date and ready for future threats of similar types. In the very first moment of facing the acute stress, an emotional response is triggered which elevates surveillance, perception, and attention on threat-related stimuli (Quaedflieg et al. 2015). Humans initially experience that they do not have the power to control the occurring stress. They are not able to change the situation and make it better (Glass et al. 1971). But it turns out that stress also has a positive effect on learning new decision making behaviour that is better adapted to the new situations encountered. To get rid of old decision making, as a first step existing connections are suppressed as a kind of reset by which more room

J. Treur, *Network-Oriented Modeling for Adaptive Networks: Designing Higher-Order Adaptive Biological, Mental and Social Network Models*, Studies in Systems, Decision and Control 251, https://doi.org/10.1007/978-3-030-31445-3_5

is created for learning new connections (Sousa and Almeida 2012); this adaptation principle is called the *disconnect-reconnect principle*. The current chapter addresses the question of how this can be modelled by a reified adaptive network model. Moreover, it is also explored how this principle works in conjunction with second-order adaptation as described by metaplasticity.

The chapter is organized as follows. In Sect. 5.2 the neurological principles of the suppressing and adaptive effects of stress and the parts of the brain which deal with stress in that way are addressed. In Sect. 5.3 the reified adaptive temporal-causal network model is introduced, and illustrated by simulation of two example scenarios in Sect. 5.4: one for the disconnect-reconnect principle without using metaplasticity and one in conjunction with metaplasticity. Section 5.5 addresses the verification of the reified network model by mathematical analysis.

5.2 Neurological Principles

Acute stress is considered to involve interaction with the amygdala (Quaedflieg et al. 2015). The more activity in the amygdala, the more a human becomes sensitive and respondent to the threat (Radley and Morrison 2005). Stress reactions on stressors often deteriorate homeostasis in organisms (de Kloet et al. 2005). But stressors also stimulate a constructive reaction which makes physiological and psychological alterations in the body that are advantageous for the organism. Recovery from a stressor is accompanied by a decreasing negative coupling between the amygdala and the frontal Anterior Cingulate Cortex (ACC) and pre-Supplementary Motor Area (preSMA) (Hermans et al. 2014). This has been found, for example, in stress-related psychiatric disorders (Etkin et al. 2010; Johnstone et al. 2007). It has been found that the left Prefrontal Cortex (PFC) is relevant to stress adaptation, and individuals with stronger Hypothalamic Pituitary Adrenal (HPA) axis reactivity show reduced amygdala-left dlPFC functional connectivity (Quaedflieg et al. 2015). In a safe environment, it is advantageous that the cortex can suppress the stress response but in a harmful environment, this may cause a false idea of security (Reser 2016). The reaction of the amygdala to new stressors makes animals behave the same as before the new stress arrived.

In Barsegyan et al. (2010), it is claimed that the executive control network is suppressed in the very starting period of the inducing of stress (by dlPFC). Stress handling is viewed as adaptive (e.g., Sousa and Almeida 2012), due to the fact that when the decision making is improved, humans can learn how to handle the situations where the stress comes from. In the case of acute stress, at the very first period of stress-induction, the salience network starts working and executive control is suppressed. After a while, executive control starts performing functionality and suppress the salience network. Due to this, plasticity, for example, based on Hebbian learning will work more efficiently; this is called the *disconnect-reconnect adaptation principle* (Sousa and Almeida 2012).

5.3 The Reified Adaptive Network Model

To simulate how stress adaptively affects decision making, the following scenario is addressed here. Person A is working (performing action a_1) in a convenient condition with her colleague B until B's context causes extreme stress for person A. This condition disturbs her normal functioning. A's brain has a neurocognitive mechanism to overcome this by learning new decision making to cope with that situation. By this mechanism, first as a form of resetting her existing connections are suppressed to create more room for new learning of connections, better adapted to the new conditions. Next, after some time, A's suppression is ending, and new Hebbian learning to cope with the new situation takes place. Finally, after this learning how to cope with the situation has led to improved decision making, person A decides for a different option (action a_2) in which B and his context do not play a dominant role anymore.

The Network-Oriented Modeling approach based on multilevel reified temporal-causal network models presented in Chap. 4 is used to model this process; see also Treur (2018a, b). Recall that a temporal-causal network model in the first place involves representing in a declarative manner states and connections between them that represent (causal) impacts of states on each other, as assumed to hold for the application domain addressed. The states are assumed to have (activation) levels in the interval [0, 1] that vary over time. These three notions form the defining part of a conceptual representation of a temporal-causal network model structure:

- **Connectivity**
  - Each incoming connection of a state Y, from a state X has a *connection weight value* $\boldsymbol{\omega}_{X,Y}$ representing the strength of the connection.
- **Aggregation**
  - For each state a *combination function* $\mathbf{c}_Y(..)$ is chosen to combine the causal impacts state Y receives from other states.
- **Timing**
  - For each state Y a *speed factor* $\boldsymbol{\eta}_Y$ is used to represent how fast state Y is changing upon causal impact.

In Figs. 5.1 and 5.2. the conceptual representation of the reified temporal-causal network model is depicted. A brief explanation of the states used is shown in Table 5.1.

5.3.1 The Base Network

The base states are as follows (see also Fig. 5.1). The state srs_s stands for the sensory representation of stimulus s from the world. The state srs_c is the sensory

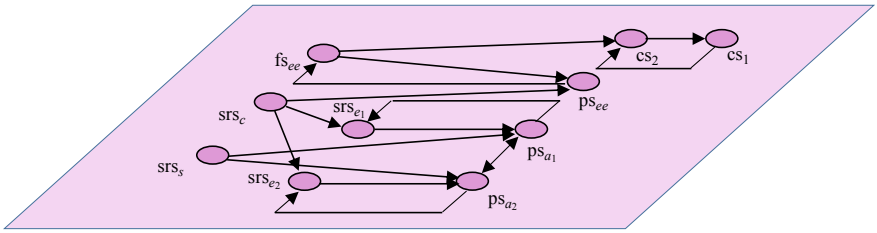

Fig. 5.1 The base network model

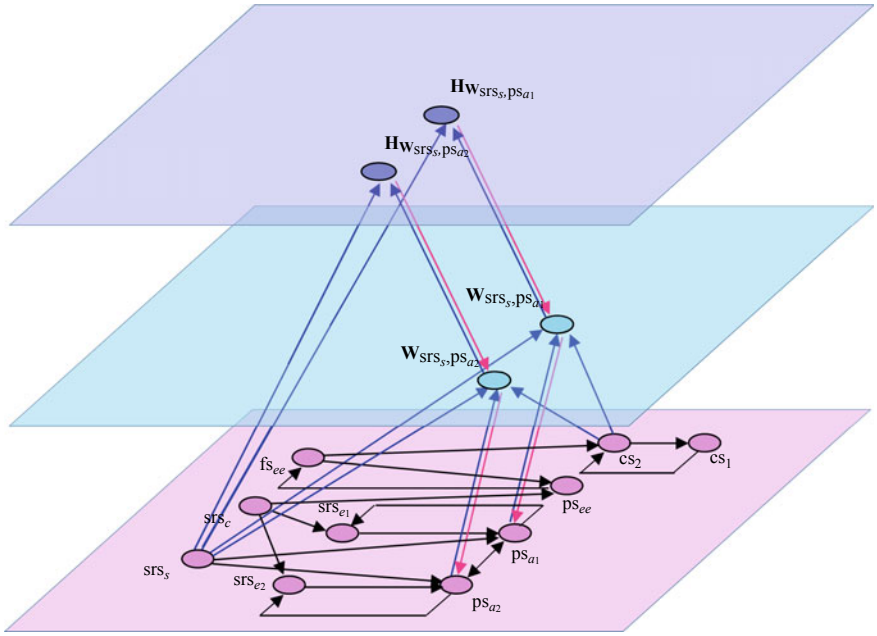

Fig. 5.2 The reified network model with plasticity and metaplasticity

representation of the stressful context c. The sensory representation srs_s of the stimulus is a trigger for the preparation state of one or both of two actions a_1 or a_2. The sensory representation of the predicted feeling effects of the preparation states ps_{a_1} and ps_{a_2} of the actions are represented by srs_{e_1} and srs_{e_2}, respectively.

Furthermore, ps_{ee} is the preparation state of a stressful emotional response on the sensory representation srs_c of the disturbing context c, and fs_{ee} denotes the feeling state associated to this extreme emotion. Finally, cs_2 stands for a control state for suppression of connections (here from srs_s to ps_{a_1} and to ps_{a_2}) and cs_1 for a control state to limit this suppression in time.

Table 5.1 Explanation of the states in the model

State nr	State name	Explanation	Level
X_1	srs_s	Sensory representation of stimulus s	Base level
X_2	srs_c	Sensory representation of context c	
X_3	srs_{e1}	Sensory representation of action effect e_1	
X_4	srs_{e2}	Sensory representation of action effect e_2	
X_5	fs_{ee}	Feeling state for extreme emotion ee	
X_6	ps_{a1}	Preparation state for action a_1	
X_7	ps_{a2}	Preparation state for action a_2	
X_8	ps_{ee}	Preparation state for response of extreme emotion ee	
X_9	cs_1	Control state for timing of suppression of connections	
X_{10}	cs_2	Control state for suppression of connections	
X_{11}	$\mathbf{W}srs_s,ps_{a_1}$	Reification state for the weight of the connection from srs_s to ps_{a1}	First reification level
X_{12}	$\mathbf{W}srs_s,ps_{a_2}$	Reification state for the weight of the connection from srs_s to ps_{a2}	
X_{13}	$\mathbf{Hw}_{srs_s,ps_{a_1}}$	Reification state for speed factor $\boldsymbol{\eta}$ of reification state $\mathbf{W}srs_s,ps_{a_1}$	Second reification level
X_{14}	$\mathbf{Hw}_{srs_s,ps_{a_2}}$	Reification state for speed factor $\boldsymbol{\eta}$ of reification state $\mathbf{W}srs_s,ps_{a_2}$	

The connections for the base network depicted in Fig. 5.1 are as follows. Preparation state ps_{a_1} has three incoming connections from srs_s, srs_{e_1}, ps_{a_2}. The first connection is for triggering preparation for action a_1, based on stimulus s. The second connection from srs_{e_1} amplifies the preparation due to a positive feeling for the predicted effect of the action. The third connection from ps_{a_2} is a negative connection to achieve that in general only one of the actions is chosen. Whether or not this action a_1 is actually chosen depends on these three connections and the activation of the three connected states. From these three connections, the connection from srs_s to ps_{a_1} is considered to be adaptive. Similarly, the other action option a_2 is handled (but with different values for the three connections). Note that by the connections from srs_c to srs_{e_1} and srs_{e_2} the stressful context c affects the predicted effects of the two actions; also these connections will have different weights as they represent how the actions differ in their suitability for this context.

The extreme stressful emotion is modeled by the as-if body loop between ps_{ee} and fs_{ee}, whereby ps_{ee} is triggered by the context representation srs_c. An effect of these stress states goes via the connection from fs_{ee} to control state cs_2. This control state is limited in its value over time by another control state cs_1 via the two mutual links; to achieve that, the connection from cs_1 to cs_2 is negative, and activation of cs_1 is slower than of cs_2.

5.3.2 *Modeling First- and Second-Order Adaptation of the Connection Weights by Reification States*

Control state cs_2 has an adaptive effect on the two network connections from srs_s in the base network. This adaptive effect combines with the Hebbian learning effect for the same adaptive connections. This is where the first reification level (see Fig. 5.2) comes in with reification states $\mathbf{W}_{srs_s,ps_{a_1}}$ and $\mathbf{W}_{srs_s,ps_{a_2}}$ for the weights of these two adaptive connections.

The blue upward links from cs_2 model the effect of cs_2 and the blue upward links from srs_s, ps_{a_1} and ps_{a_2} model the Hebbian learning on the same connections. The pink downward links from the reification states model the effect of the adaptive connection weights on ps_{a_1} and ps_{a_2}.

Yet another adaptive effect is modeled by the second reification level in Fig. 5.2. This is a form of metaplasticity that increases the adaptation speed of the two adaptive connection weights, which is triggered by experiencing srs_s; also see: 'Adaptation accelerates with increasing stimulus exposure' (Robinson et al. 2016, p. 2). Second-order reification states $\mathbf{H}_{\mathbf{W}_{srs_s,ps_{a_1}}}$ and $\mathbf{H}_{\mathbf{W}_{srs_s,ps_{a_2}}}$ achieve this second-order effect, using the upward blue links from srs_s and the downward pink links to $\mathbf{W}_{srs_s,ps_{a_1}}$ and $\mathbf{W}_{srs_s,ps_{a_2}}$.

5.4 Combination Functions and Role Matrices for the Reified Network Model

In this section, first, the combination functions used are discussed. Next, the role matrices are presented.

5.4.1 *The Combination Functions Used*

For base states the following combination functions $\mathbf{c}_Y(\ldots)$ were used:

$$\mathbf{ssum}_{\boldsymbol{\lambda}}(V_1,\ldots,V_k) = \frac{V_1+\cdots+V_k}{\boldsymbol{\lambda}} \tag{5.1}$$

$$\mathbf{eucl}_{n,\boldsymbol{\lambda}}(V_1,\ldots,V_k) = \sqrt[n]{\frac{V_1^n+\cdots+V_k^n}{\boldsymbol{\lambda}}} \tag{5.2}$$

$$\mathbf{alogistic}_{\boldsymbol{\sigma},\boldsymbol{\tau}}(V_1,\ldots V_k) = \left[\frac{1}{1+\mathrm{e}^{-\boldsymbol{\sigma}(V_1+\cdots+V_k-\boldsymbol{\tau})}} - \frac{1}{1+\mathrm{e}^{\boldsymbol{\sigma}\boldsymbol{\tau}}}\right](1+\mathrm{e}^{-\boldsymbol{\sigma}\boldsymbol{\tau}}) \tag{5.3}$$

Similarly, for the reification states of the connection weights, the following two combination functions were used. *Hebbian learning* of a connection from state X_i to state X_j with connection weight reification state **W** makes use of:

$$\mathbf{hebb}_{\boldsymbol{\mu}}(V_1, V_2, W) = V_1 V_2 (1-W) + \boldsymbol{\mu}\, W \tag{5.4}$$

where $\boldsymbol{\mu}$ is the persistence factor with value 1 as full persistence and 0 as none. For *state-connection modulation* with control state cs_2 for connection weight reification state **W**:

$$\mathbf{scm}_{\boldsymbol{\alpha}}(V_1, V_2, W, V) = W + \boldsymbol{\alpha}\, V\, W(1-W) \tag{5.5}$$

where $\boldsymbol{\alpha}$ (or $\boldsymbol{\alpha}_{cs_2,\mathbf{W}}$) is the modulation parameter for **W** from cs_2, and V is the single impact from cs_2. Note that the first two variables of $\mathbf{scm}_{\boldsymbol{\alpha}}(V_1, V_2, W, V)$ are auxiliary variables that are not used in Formula (5) for $\mathbf{scm}_{\boldsymbol{\alpha}}(V_1, V_2, W, V)$. These auxiliary variables are included to be able to combine this function with the Hebbian learning function while using the same sequence of variables (see 6 below). More specifically, this combination is done as follows. These two adaptive combination functions are used as a weighted average with $\boldsymbol{\gamma_1}$ and $\boldsymbol{\gamma_2}$ as combination function weights (with sum 1) for $\mathbf{hebb}_{\boldsymbol{\mu}}(V_1, V_2, W)$ and $\mathbf{scm}_{\boldsymbol{\alpha}}(V_1, V_2, W, V)$, respectively, based on (4) and (5) as follows:

$$\mathbf{c}_{\mathbf{W}}(V_1, V_2, W, V) = \boldsymbol{\gamma_1}\mathbf{hebb}_{\boldsymbol{\mu}}(V_1, V_2, W) + \boldsymbol{\gamma_2}\mathbf{scm}_{\boldsymbol{\alpha}}(V_1, V_2, W, V) \tag{5.6}$$

5.4.2 The Role Matrices

Based on the graphical representations from Fig. 5.2 and the specific values for the intended scenario the role matrices shown in Boxes 5.1 and 5.2 have been specified. Note that the reification states $\mathbf{W}_{\mathrm{srs}_s,\mathrm{ps}_{a_1}}$ and $\mathbf{W}_{\mathrm{srs}_s,\mathrm{ps}_{a_2}}$ for the connection weights also have a connection to themselves, as can be seen in role matrix **mb**. This is because Hebbian learning needs that; these connections are not shown in Fig. 5.2.

Box 5.1 Role matrices **mb** for base connections, **mcw** for connection weights, **mcfw** for combination function weights, and **mcfp** for combination function parameters.

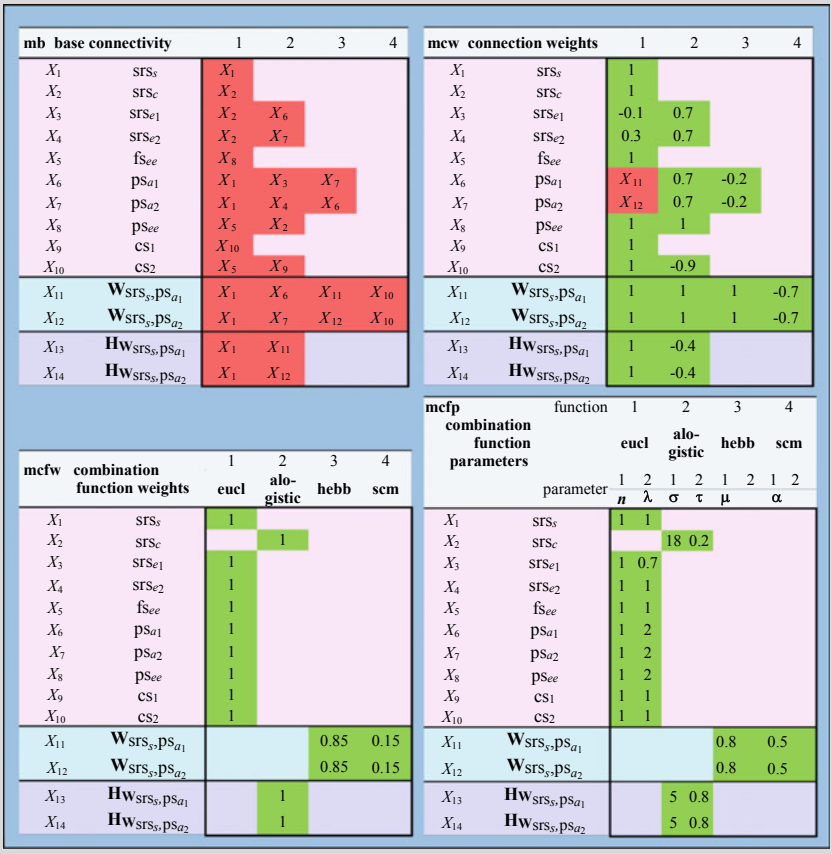

mb	base connectivity	1	2	3	4
X_1	srs_s	X_1			
X_2	srs_c	X_2			
X_3	srs_{e1}	X_2	X_6		
X_4	srs_{e2}	X_2	X_7		
X_5	fs_{ee}	X_8			
X_6	ps_{a1}	X_1	X_3	X_7	
X_7	ps_{a2}	X_1	X_4	X_6	
X_8	ps_{ee}	X_5	X_2		
X_9	cs_1	X_{10}			
X_{10}	cs_2	X_5	X_9		
X_{11}	$\mathbf{W}_{srs_s,ps_{a_1}}$	X_1	X_6	X_{11}	X_{10}
X_{12}	$\mathbf{W}_{srs_s,ps_{a_2}}$	X_1	X_7	X_{12}	X_{10}
X_{13}	$\mathbf{Hw}_{srs_s,ps_{a_1}}$	X_1	X_{11}		
X_{14}	$\mathbf{Hw}_{srs_s,ps_{a_2}}$	X_1	X_{12}		

mcw	connection weights	1	2	3	4
X_1	srs_s	1			
X_2	srs_c	1			
X_3	srs_{e1}	-0.1	0.7		
X_4	srs_{e2}	0.3	0.7		
X_5	fs_{ee}	1			
X_6	ps_{a1}	X_{11}	0.7	-0.2	
X_7	ps_{a2}	X_{12}	0.7	-0.2	
X_8	ps_{ee}	1	1		
X_9	cs_1	1			
X_{10}	cs_2	1	-0.9		
X_{11}	$\mathbf{W}_{srs_s,ps_{a_1}}$	1	1	1	-0.7
X_{12}	$\mathbf{W}_{srs_s,ps_{a_2}}$	1	1	1	-0.7
X_{13}	$\mathbf{Hw}_{srs_s,ps_{a_1}}$	1	-0.4		
X_{14}	$\mathbf{Hw}_{srs_s,ps_{a_2}}$	1	-0.4		

mcfw	combination function weights	1 eucl	2 alo-gistic	3 hebb	4 scm
X_1	srs_s	1			
X_2	srs_c		1		
X_3	srs_{e1}	1			
X_4	srs_{e2}	1			
X_5	fs_{ee}	1			
X_6	ps_{a1}	1			
X_7	ps_{a2}	1			
X_8	ps_{ee}	1			
X_9	cs_1	1			
X_{10}	cs_2	1			
X_{11}	$\mathbf{W}_{srs_s,ps_{a_1}}$			0.85	0.15
X_{12}	$\mathbf{W}_{srs_s,ps_{a_2}}$			0.85	0.15
X_{13}	$\mathbf{Hw}_{srs_s,ps_{a_1}}$		1		
X_{14}	$\mathbf{Hw}_{srs_s,ps_{a_2}}$		1		

mcfp	combination function parameters	function	1 eucl		2 alo-gistic			3 hebb		4 scm	
		parameter	1 n	2 λ	1 σ	2 τ		1 μ	2	1 α	2
X_1	srs_s		1	1							
X_2	srs_c				18	0.2					
X_3	srs_{e1}		1	0.7							
X_4	srs_{e2}		1	1							
X_5	fs_{ee}		1	1							
X_6	ps_{a1}		1	2							
X_7	ps_{a2}		1	2							
X_8	ps_{ee}		1	2							
X_9	cs_1		1	1							
X_{10}	cs_2		1	1							
X_{11}	$\mathbf{W}_{srs_s,ps_{a_1}}$							0.8		0.5	
X_{12}	$\mathbf{W}_{srs_s,ps_{a_2}}$							0.8		0.5	
X_{13}	$\mathbf{Hw}_{srs_s,ps_{a_1}}$				5	0.8					
X_{14}	$\mathbf{Hw}_{srs_s,ps_{a_2}}$				5	0.8					

In matrix **mcfw** in Box 5.1, it is indicated which states get which combination functions. As shown, almost all base states get the Euclidean combination function. The only exception is state srs_c which only has a link to itself. The chosen logistic sum combination function allows to get some pattern over time for the environment in which the stressor occurs after some time. Also the second-order reification states $\mathbf{H}_{\mathbf{W}_{srs_s,ps_{a_1}}}$ and $\mathbf{H}_{\mathbf{W}_{srs_s,ps_{a_2}}}$ have a logistic combination function. Note that the first-order reification states $\mathbf{W}_{srs_s,ps_{a_1}}$ and $\mathbf{W}_{srs_s,ps_{a_2}}$ get a weighted average (with weights $\boldsymbol{\gamma_1} = 0.85$ and $\boldsymbol{\gamma_2} = 0.15$) of two combination functions: $\mathbf{hebb}_{\boldsymbol{\mu}}(..)$ for

Hebbian learning, and **scm$_\alpha$(..)** for state-connection modulation as described in (6) above. All other states have single combination functions. In role matrix **mcfp** the parameter values for the chosen combination functions are shown. As can be seen, all Euclidean combination functions have order 1, which actually makes them scaled sum functions.

Box 5.2 Role matrix **ms** for speed factors and vector **iv** of initial values.

ms	**speed factors**	1
X_1	srs_s	0
X_2	srs_c	0.05
X_3	srs_{e1}	0.5
X_4	srs_{e2}	0.5
X_5	fs_{ee}	0.5
X_6	ps_{a1}	0.5
X_7	ps_{a2}	0.5
X_8	ps_{ee}	0.5
X_9	cs1	0.02
X_{10}	cs2	0.6
X_{11}	$\mathbf{W}\mathrm{srs}_s,\mathrm{ps}_{a1}$	X_{13}
X_{12}	$\mathbf{W}\mathrm{srs}_s,\mathrm{ps}_{a2}$	X_{14}
X_{13}	$\mathbf{Hw}\mathrm{srs}_s,\mathrm{ps}_{a1}$	0.5
X_{14}	$\mathbf{Hw}\mathrm{srs}_s,\mathrm{ps}_{a2}$	0.5

iv	**initial values**	1
X_1	srs_s	1
X_2	srs_c	0.1
X_3	srs_{e1}	0
X_4	srs_{e2}	0
X_5	fs_{ee}	0
X_6	ps_{a1}	0
X_7	ps_{a2}	0
X_8	ps_{ee}	0
X_9	cs1	0
X_{10}	cs2	0
X_{11}	$\mathbf{W}\mathrm{srs}_s,\mathrm{ps}_{a1}$	0.9
X_{12}	$\mathbf{W}\mathrm{srs}_s,\mathrm{ps}_{a2}$	0.3
X_{13}	$\mathbf{Hw}\mathrm{srs}_s,\mathrm{ps}_{a1}$	0.05
X_{14}	$\mathbf{Hw}\mathrm{srs}_s,\mathrm{ps}_{a2}$	0.05

In Box 5.2 the speed factors and the initial values for the chosen scenario are shown. Note that initially the weight of the incoming connection for action a_1 is high and for a_2 low. This models that initially the preferred action is a_1.

5.5 Example Simulation Scenarios

Two example simulation scenarios of this process are shown in Figs. 5.3, 5.4, 5.5 and 5.6. Boxes 5.1 and 5.2 show the reified network characteristics used. The step size was $\Delta t = 0.4$. In the two scenarios, coping with an extremely stressful condition c (disturbing context due to person B) takes place. The trigger for doing one of the actions is the sensory representation state srs_s (also denoted by X_1), which has value 1 all the time. In the first scenario, only first-order adaptation takes place according to the disconnect-reconnect principle (Sousa and Almeida 2012). In the second scenario, in addition, also metaplasticity is assumed, which leads to second-order adaptation.

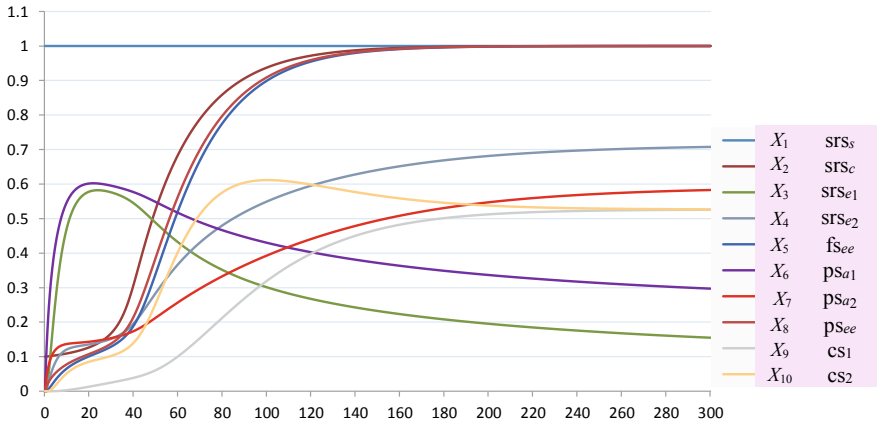

Fig. 5.3 Simulation results of working under an extremely stressful condition without metaplasticity: base states

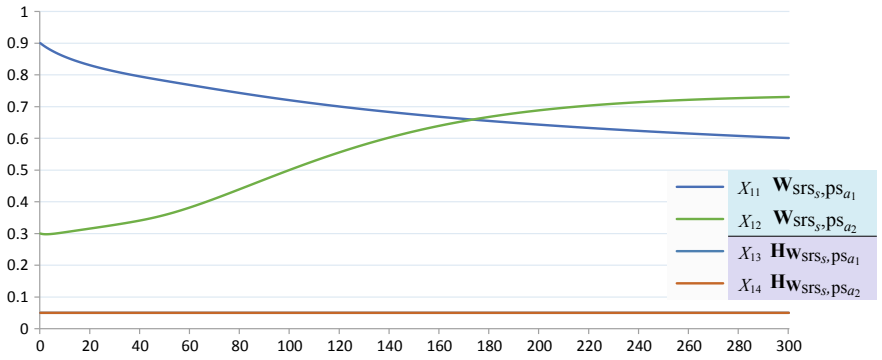

Fig. 5.4 Simulation results for state-connection modulation and Hebbian learning (without metaplasticity) for X_{11} (connection weight reification $\mathbf{W}_{srs_s,ps_{a_1}}$) and X_{12} (connection weight reification $\mathbf{W}_{srs_s,ps_{a_2}}$)

5.5.1 *Scenario 1: First-Order Adaptation; No Adaptive Speed of Connection Weight Change*

In Scenario 1, the speed factors for the second-order reification states for metaplasticity have been set at 0, so that the speed of adaptation of the connection weights $\mathbf{W}_{srs_s,ps_{a_1}}$ (X_{11}) and $\mathbf{W}_{srs_s,ps_{a_2}}$ (X_{12}) was constant, equal to the initial values 0.05. Note that the initial preference for action a_1 over a_2 is shown by a high initial value 0.9 for $\mathbf{W}_{srs_s,ps_{a_1}}$ (X_{11}) and a low initial value 0.3 for $\mathbf{W}_{srs_s,ps_{a_2}}$ (X_{12}); see Fig. 5.4. At the early time of working, there is a convenient condition in the working place. Therefore, as can be seen in Fig. 5.3, srs_c (also denoted by X_2) has a

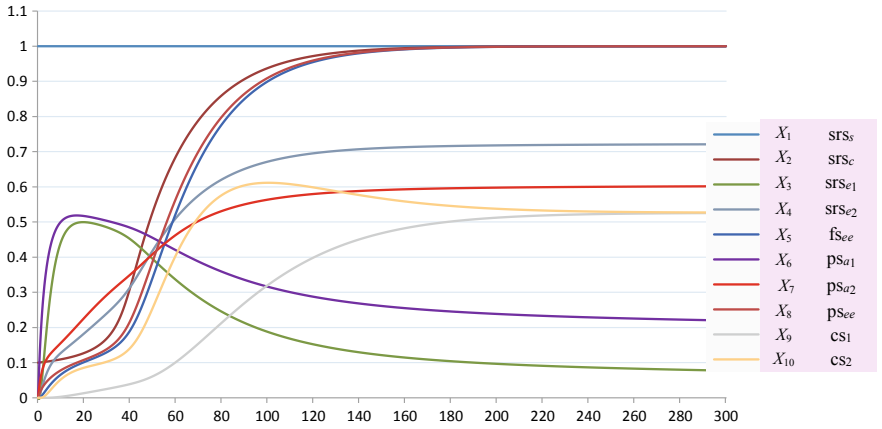

Fig. 5.5 Simulation results of working under an extremely stressful condition with metaplasticity: base states

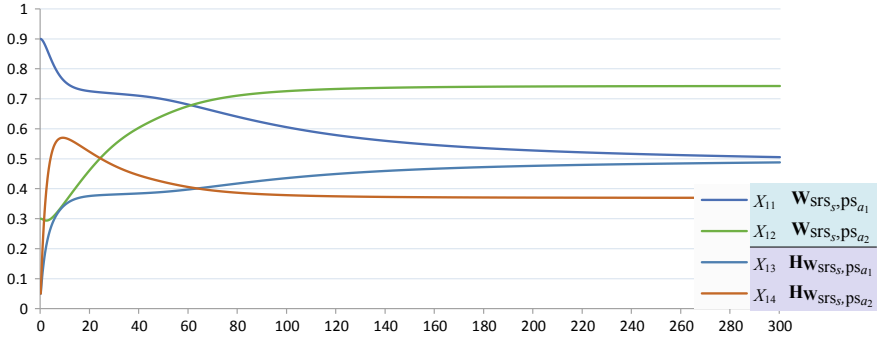

Fig. 5.6 Simulation results for state-connection modulation and Hebbian learning (with metaplasticity) for X_{11} (connection weight reification $\mathbf{W}_{srs_s,ps_{a_1}}$) and X_{12} (connection weight reification $\mathbf{W}_{srs_s,ps_{a_2}}$)

low value, which, however, strongly increases after some time (around time point 30 in Fig. 5.3) when the disturbances start.

Sensory representation state srs_{e_1} (X_3) shows that person A initially has a good feeling for the effect of action a_1, which strengthens the preparation ps_{a_1} (X_6) for this action in the first phase; see the purple line in Fig. 5.3 that steeply goes up to 0.6. However, after time point 30 when the acute stress occurs, this changes. Both the feeling srs_{e_1} for the action effect and the preparation ps_{a_1} for the action a_1 drop. Moreover, after this time point control state cs_2 (X_{10}), which stands for the control state for suppression of the connections, starts to go up but after some time the other control state cs_1 (X_9) in turn begins to play a role in suppressing cs_2. Therefore, the actual suppression of the connections mainly takes place between

time points 50 and 150. During that time due to the acute stress, the control state cs_2 has a suppressing effect on the two reification states $\mathbf{W}_{srs_s,ps_{a_1}}$ (X_{11}) and $\mathbf{W}_{srs_s,ps_{a_2}}$ (X_{12}) for the adaptive connections, which is illustrated in the graphs of these two reification states in Fig. 5.4.

After some time the suppression is released, and by the Hebbian learning, the person develops another decision to cope with her task under the extremely stressful condition c. This is shown by increased activation of preparation state ps_{a_2} (X_7), shown as the red line in Fig. 5.3, and by an increasing $\mathbf{W}_{srs_s,ps_{a_2}}$ (X_{12}, for the connection X_1–X_7) in Fig. 5.4, in contrast to the decrease of $\mathbf{W}_{srs_s,ps_{a_1}}$ (for connection X_1–X_6). Due to this, now the action a_2 becomes dominating. This illustrates the working of the disconnect-reconnect adaptation principle of Sousa and Almeida (2012).

5.5.2 *Scenario 2: Second-Order Adaptation; Adaptive Speed of Connection Weight Change*

In this second scenario, the speed factors of the connection weight adaptation are themselves adaptive, so there is second-order adaptation. As in Scenario 1, it can be seen in Fig. 5.5 that also for Scenario 2 after a while action a_2 becomes dominant over a_1. However, as can be seen in Fig. 5.6, the change of the connection weights is much earlier, so now after time point 60 the connection to ps_{a_2} is already stronger than the connection to ps_{a_1}, whereas in Scenario 1 that point was only reached after time point 180; see Fig. 5.4. This has also effect on the pattern for ps_{a_1} and ps_{a_2} in Fig. 5.5. In Scenario 2, ps_{a_2} is already stronger than ps_{a_1} after time point 60, whereas in Scenario 1 this is only the case after time point 110. So, in both cases the initial preference for action a_1 changes to a preference for action a_2, but due to the second-order adaptation, this adaptation happens much faster in Scenario 2, which is an advantage in urgent, stressful situations. This illustrates once more the relevance of second-order adaptation or metaplasticity.

5.6 Verification of the Network Model by Mathematical Analysis

For temporal-causal network models, dedicated methods have been developed enabling to verify whether the implemented model shows behavior as expected; see Treur (2016a) or Treur (2016b), Chap. 12. In this section, in particular, the focus is on equilibria: they are determined by Mathematical Analysis and then used for verification by comparison to simulation results. First a definition

Definition (stationary point and equilibrium)
A state Y in an adaptive temporal-causal network model has a *stationary point* at t if $\mathbf{d}Y(t)/\mathbf{d}t = 0$.
A temporal-causal network model is in an *equilibrium state* at t if all states have a stationary point at t.
In that case, the above equations $\mathbf{d}Y(t)/\mathbf{d}t = 0$ for all states Y provide the *equilibrium equations*.

The above definition is quite general. However, for adaptive temporal-causal network models the following simple criterion was obtained in terms of the basic characteristics defining the network structure, in particular (besides the states X_i and Y), speed factor $\boldsymbol{\eta}_Y$, connection weights $\boldsymbol{\omega}$ and the combination function $\mathbf{c}(..)$; see Treur, (2016a) or Treur, (2016b), Chap. 12.

Criterion for stationary points and equilibria in temporal-causal network models A state Y in an adaptive temporal-causal network model has a stationary point at t if and only if

$$\boldsymbol{\eta}_Y = 0 \quad \text{or} \quad \mathbf{c}_Y(\boldsymbol{\omega}_{X_1,Y}(t)X_1(t), \ldots, \boldsymbol{\omega}_{X_k,Y}(t)X_k(t)) = Y(t)$$

where X_1, …, X_k are the states with outgoing connections to Y.

An adaptive temporal-causal network model is in an equilibrium state at t if and only if for all states with nonzero speed factor, the above criteria hold at t.

Note that in the case of reification of characteristics $\boldsymbol{\eta}_Y$, $\boldsymbol{\omega}_{X_k,Y}$, $\mathbf{c}_Y(..)$ that occur in this criterion, in principle, the universal combination function $\mathbf{c}^*_Y(..)$ and the related difference equation has to be considered. However, the universal differential equation can be written in the following form, as has been mentioned in Chap. 3, Sect. 3.5 (for more details, see also Chap. 10, Sect. 10.4.2 and 10.5):

$$\mathbf{d}Y/\mathbf{d}t = \mathbf{H}_Y\left[\frac{\mathbf{C}_{1,Y}\mathrm{bcf}_1(\mathbf{P}_{1,1,Y}, \mathbf{P}_{2,1,Y}, \mathbf{W}_{X_1,Y}X_1, \ldots, \mathbf{W}_{X_k,Y}X_k) + \cdots + \mathbf{C}_{m,Y}\mathrm{bcf}_m(\mathbf{P}_{1,m,Y}, \mathbf{P}_{2,m,Y}, \mathbf{W}_{X_1,Y}X_1, \ldots, \mathbf{W}_{X_k,Y}X_k)}{\mathbf{C}_{1,Y} + \cdots + \mathbf{C}_{m,Y}} - Y\right]$$

The right hand side of this is 0 if and only if

$$\mathbf{H}_Y = 0 \quad \text{or} \quad \frac{\mathbf{C}_{1,Y}\mathrm{bcf}_1(\mathbf{P}_{1,1,Y}, \mathbf{P}_{2,1,Y}, \mathbf{W}_{X_1,Y}X_1, \ldots, \mathbf{W}_{X_k,Y}X_k) + \cdots + \mathbf{C}_{m,Y}\mathrm{bcf}_m(\mathbf{P}_{1,m,Y}, \mathbf{P}_{2,m,Y}, \mathbf{W}_{X_1,Y}X_1, \ldots, \mathbf{W}_{X_k,Y}X_k)}{\mathbf{C}_{1,Y} + \cdots + \mathbf{C}_{m,Y}} = Y$$

where the left-hand side is the combination function. This shows that the above criterion also can be used when some or all characteristics are adaptive.

5.6.1 Solving the Linear Equilibrium Equations for the Base Network

The criterion for an equilibrium for a scaled sum function

$$\mathbf{c}_Y(\boldsymbol{\omega}_{X_1,Y}(t)X_1(t),\ldots,\boldsymbol{\omega}_{X_k,Y}(t)X_k(t)) = (\boldsymbol{\omega}_{X_1,Y}(t)X_1(t)+\cdots+\boldsymbol{\omega}_{X_k,Y}(t)X_k(t))/\boldsymbol{\lambda}_Y = Y(t) \tag{5.7}$$

provides a linear equilibrium equation (leaving out t):

$$\boldsymbol{\omega}_{X_1,Y}X_1+\cdots+\boldsymbol{\omega}_{X_k,Y}X_k = \boldsymbol{\lambda}_Y Y \tag{5.8}$$

in the state values $X_i(t)$ and $Y(t)$ involved. In this way for the network model introduced here the equilibrium equations for the states were obtained as shown in Box 5.3, where the values for srs_s and srs_c are indicated by A_1 and A_2 (here to simplify notation the reference to t has been left out, and underlining is used to indicate that this concerns state values, not state names). Moreover, the scaling factor for state X_i is denoted by $\boldsymbol{\lambda}_i$, and in Table 5.2 numbered connection weight names are indicated.

Then the linear equilibrium equations are obtained as shown in Box 5.3, in the left half in terms of the informative state names, and in the right half in terms of the numbered X_i as state names; see Table 5.1.

Box 5.3 General equilibrium equations for the base network

$\underline{\text{srs}}_s = A_1$	$X_1 = A_1$
$\underline{\text{srs}}_c = A_2$	$X_2 = A_2$
$\boldsymbol{\lambda}_3\underline{\text{srs}}_{e_1} = \boldsymbol{\omega}_7\underline{\text{ps}}_{a_1} + \boldsymbol{\omega}_9\underline{\text{srs}}_c$	$\boldsymbol{\lambda}_3X_3 = \boldsymbol{\omega}_7X_6 + \boldsymbol{\omega}_9X_2$
$\boldsymbol{\lambda}_4\underline{\text{srs}}_{e_2} = \boldsymbol{\omega}_8\underline{\text{ps}}_{a_2} + \boldsymbol{\omega}_{10}\underline{\text{srs}}_c$	$\boldsymbol{\lambda}_4X_4 = \boldsymbol{\omega}_8X_7 + \boldsymbol{\omega}_{10}X_2$
$\underline{\text{fs}}_{ee} = \boldsymbol{\omega}_{13}\underline{\text{ps}}_{ee}$	$X_5 = \boldsymbol{\omega}_{13}X_8$
$\boldsymbol{\lambda}_6\underline{\text{ps}}_{a_1} = \boldsymbol{\omega}_1\underline{\text{srs}}_s + \boldsymbol{\omega}_3\underline{\text{srs}}_{e_1} + \boldsymbol{\omega}_5\underline{\text{ps}}_{a_2}$	$\boldsymbol{\lambda}_6X_6 = \boldsymbol{\omega}_1X_1 + \boldsymbol{\omega}_3X_3 + \boldsymbol{\omega}_5X_7$
$\boldsymbol{\lambda}_7\underline{\text{ps}}_{a_2} = \boldsymbol{\omega}_2\underline{\text{srs}}_s + \boldsymbol{\omega}_4\underline{\text{srs}}_{e_2} + \boldsymbol{\omega}_6\underline{\text{ps}}_{a_1}$	$\boldsymbol{\lambda}_7X_7 = \boldsymbol{\omega}_2X_1 + \boldsymbol{\omega}_4X_4 + \boldsymbol{\omega}_6X_6$
$\boldsymbol{\lambda}_8\underline{\text{ps}}_{ee} = \boldsymbol{\omega}_{11}\underline{\text{srs}}_c + \boldsymbol{\omega}_{12}\underline{\text{fs}}_{ee}$	$\boldsymbol{\lambda}_8X_8 = \boldsymbol{\omega}_{11}X_2 + \boldsymbol{\omega}_{12}X_5$
$\underline{\text{cs}}_1 = \boldsymbol{\omega}_{14}\underline{\text{cs}}_2$	$X_9 = \boldsymbol{\omega}_{14}X_{10}$
$\boldsymbol{\lambda}_{10}\underline{\text{cs}}_2 = \boldsymbol{\omega}_{15}\underline{\text{fs}}_{ee} + \boldsymbol{\omega}_{16}\underline{\text{cs}}_1$	$\boldsymbol{\lambda}_{10}X_{10} = \boldsymbol{\omega}_{15}X_5 + \boldsymbol{\omega}_{16}X_9$

Table 5.2 Numbering of connection weights

From	To	Connection weight	From	To	Connection weight
srs_s	ps_{a_1}	ω_1	srs_c	srs_{e_1}	ω_9
srs_s	ps_{a_2}	ω_2	srs_c	srs_{e_2}	ω_{10}
srs_{e_1}	ps_{a_1}	ω_3	srs_c	ps_{ee}	ω_{11}
srs_{e_2}	ps_{a_2}	ω_4	fs_{ee}	ps_{ee}	ω_{12}
ps_{a_2}	ps_{a_1}	ω_5	ps_{ee}	fs_{ee}	ω_{13}
ps_{a_1}	ps_{a_2}	ω_6	fs_{ee}	cs_2	ω_{14}
ps_{a_1}	srs_{e_1}	ω_7	cs_2	cs_1	ω_{15}
ps_{a_2}	srs_{e_2}	ω_8	cs_1	cs_2	ω_{16}

Using the WIMS Linear Solver,[1] the (unique) algebraic solution was obtained for the general case of these equations as shown in Box 5.4.

Box 5.4 General solution of the equilibrium equations for the base network as generated by the WIMS Linear Solver (see Footnote 1)

$$
\begin{aligned}
X_1 &= A_1\\
X_2 &= A_2\\
X_3 &= -(A_2(\lambda_6(\lambda_4\lambda_7\omega_9 - \omega_4\omega_8\omega_9) + \omega_5(\omega_{10}\omega_4\omega_7 - \lambda_4\omega_6\omega_9))\\
&\quad + A_1(\omega_1(\lambda_4\lambda_7\omega_7 - \omega_4\omega_7\omega_8) + \lambda_4\omega_2\omega_5\omega_7))\\
&\quad /(\omega_3(\lambda_4\lambda_7\omega_7 - \omega_4\omega_7\omega_8) + \lambda_6(\lambda_3\omega_4\omega_8 - \lambda_3\lambda_4\lambda_7) + \lambda_3\lambda_4\omega_5\omega_6)\\
X_4 &= (A_2(\omega_3(\lambda_7\omega_{10}\omega_7 - \omega_6\omega_8\omega_9) + \lambda_3\omega_{10}\omega_5\omega_6 - \lambda_3\lambda_6\lambda_7\omega_{10})\\
&\quad + A_1(\omega_2\omega_3\omega_7\omega_8 - \lambda_3\omega_1\omega_6\omega_8 - \lambda_3\lambda_6\omega_2\omega_8))\\
&\quad /(\omega_3(\lambda_4\lambda_7\omega_7 - \omega_4\omega_7\omega_8) + \lambda_6(\lambda_3\omega_4\omega_8 - \lambda_3\lambda_4\lambda_7) + \lambda_3\lambda_4\omega_5\omega_6)\\
X_5 &= -A_2\omega_{11}\omega_{13}/(\omega_{12}\omega_{13} - \lambda_8)\\
X_6 &= -(A_2(\omega_3(\lambda_4\lambda_7\omega_9 - \omega_4\omega_8\omega_9) + \lambda_3\omega_{10}\omega_4\omega_5)\\
&\quad + A_1(\omega_1(\lambda_3\lambda_4\lambda_7 - \lambda_3\omega_4\omega_8) + \lambda_3\lambda_4\omega_2\omega_5))\\
&\quad /(\omega_3(\lambda_4\lambda_7\omega_7 - \omega_4\omega_7\omega_8) + \lambda_6(\lambda_3\omega_4\omega_8 - \lambda_3\lambda_4\lambda_7) + \lambda_3\lambda_4\omega_5\omega_6)\\
X_7 &= (A_2(\omega_3(\omega_{10}\omega_4\omega_7 - \lambda_4\omega_6\omega_9) - \lambda_3\lambda_6\omega_{10}\omega_4)\\
&\quad + A_1(\lambda_4\omega_2\omega_3\omega_7 - \lambda_3\lambda_4\omega_1\omega_6 - \lambda_3\lambda_4\lambda_6\omega_2))\\
&\quad /(\omega_3(\lambda_4\lambda_7\omega_7 - \omega_4\omega_7\omega_8) + \lambda_6(\lambda_3\omega_4\omega_8 - \lambda_3\lambda_4\lambda_7) + \lambda_3\lambda_4\omega_5\omega_6)
\end{aligned}
$$

[1] https://wims.unice.fr/wims/wims.cgi?session=K06C12840B.2&+lang=nl&+module=tool%2Flinear%2Flinsolver.en.

$$X_8 = -A_2\boldsymbol{\omega}_{11}/(\boldsymbol{\omega}_{12}\boldsymbol{\omega}_{13} - \boldsymbol{\lambda}_8)$$
$$X_9 = A_2\boldsymbol{\omega}_{11}\boldsymbol{\omega}_{13}\boldsymbol{\omega}_{14}\boldsymbol{\omega}_{15}/(\boldsymbol{\omega}_{12}\boldsymbol{\omega}_{13}(\boldsymbol{\omega}_{14}\boldsymbol{\omega}_{16} - \boldsymbol{\lambda}_{10}) + \boldsymbol{\lambda}_8(\boldsymbol{\lambda}_{10} - \boldsymbol{\omega}_{14}\boldsymbol{\omega}_{16}))$$
$$X_{10} = A_2\boldsymbol{\omega}_{11}\boldsymbol{\omega}_{13}\boldsymbol{\omega}_{15}/(\boldsymbol{\omega}_{12}\boldsymbol{\omega}_{13}(\boldsymbol{\omega}_{14}\boldsymbol{\omega}_{16} - \boldsymbol{\lambda}_{10}) + \boldsymbol{\lambda}_8(\boldsymbol{\lambda}_{10} - \boldsymbol{\omega}_{14}\boldsymbol{\omega}_{16}))$$

To compare these outcomes with simulation outcomes, in particular, the ones depicted in Figs. 5.3 and 5.4, that specific scenario has been addressed, with parameter values as indicated in Sect. 4, and $A_1 = A_2 = 1$.

$$X_1 = 1 \qquad X_6 = -0.1040\underline{\boldsymbol{\omega}}_2 + 0.7852\underline{\boldsymbol{\omega}}_1 - 0.1004$$
$$X_2 = 1 \qquad X_7 = 0.6760\underline{\boldsymbol{\omega}}_2 - 0.1040\underline{\boldsymbol{\omega}}_1 + 0.1524$$
$$X_3 = -0.1040\underline{\boldsymbol{\omega}}_2 + 0.7852\underline{\boldsymbol{\omega}}_1 - 0.2432 \qquad X_8 = 1$$
$$X_4 = 0.4732\underline{\boldsymbol{\omega}}_2 - 0.07280\underline{\boldsymbol{\omega}}_1 + 0.4067 \qquad X_9 = 0.5263$$
$$X_5 = 1 \qquad X_{10} = 0.5263$$

Now, from the simulation it turns out that in the equilibrium state $\boldsymbol{\omega}_1 = 0.5025559926$ and $\boldsymbol{\omega}_2 = 0.7428984649$. Substituting this in the above expressions provides:

$$X_1 = 1 \quad X_3 = 0.0741 \quad X_5 = 1 \quad X_7 = 0.6023 \quad X_9 = 0.5263$$
$$X_2 = 1 \quad X_4 = 0.7216 \quad X_6 = 0.2170 \quad X_8 = 1 \quad X_{10} = 0.5263$$

For verification, these state values found by analysis have been compared (in more precision) with the equilibrium state values found in the simulation for $\Delta t = 0.25$. The results are shown in Table 5.3. As can be seen, all deviations (differences between value from the simulation and value from the analysis) are in absolute value less than 0.001, which provides evidence that the model does what is expected.

Table 5.3 Comparing analysis and simulation

State	srs_s X_1	srs_c X_2	srs_{e_1} X_3	srs_{e_2} X_4	fs_{ee} X_5
Simulation	1.0000000000	0.9999866365	0.0750260707	0.7214675588	0.9999771825
Analysis	1.0000000000	1.0000000000	0.0741370620	0.7216223422	1.0000000000
Deviation	0	−1.33635E−05	0.000889009	0.000154783	−2.28175E-05
State	ps_{a_1} X_6	ps_{a_2} X_7	ps_{ee} X_8	cs_1 X_9	cs_2 X_{10}
Simulation	0.2175996003	0.6021532734	0.9999794070	0.5257977548	0.5267889246
Analysis	0.2169942048	0.6023176317	1.0000000000	0.5263157895	0.5263157895
Deviation	0.000605395	−0.000164358	−2.0593E−05	−0.000518035	0.000473135

5.6.2 Addressing the Nonlinear Equilibrium Equations for the Reification States

Also for the two reification states $\mathbf{W}_{\mathrm{srs}_s,\mathrm{ps}_{a_1}}$ (now indicated by $\mathbf{W}_1$ with value W_1) and $\mathbf{W}_{\mathrm{srs}_s,\mathrm{ps}_{a_2}}$ (now indicated by $\mathbf{W}_2$ with value W_2) for the two adaptive connection weights equilibrium equations can be found. They are (as long as the speed factor of them is not 0):

$$\begin{aligned} W_1 &= c_{\mathbf{W}_1}(X_1, X_6, W_1, -0.7\,\mathrm{cs}_2) \\ W_2 &= c_{\mathbf{W}_2}(X_1, X_7, W_2, -0.7\,\mathrm{cs}_2) \end{aligned} \tag{5.9}$$

Or in terms of X_i:

$$\begin{aligned} X_{11} &= c_{\mathbf{W}_1}(X_1, X_6, X_{11}, -0.7\,X_{10}) \\ X_{12} &= c_{\mathbf{W}_2}(X_1, X_7, X_{12}, -0.7\,X_{10}) \end{aligned}$$

Filling in $\mathrm{c}_{\mathbf{W}_1}(..)$ and $\mathrm{c}_{\mathbf{W}_2}(..)$ the two combination functions $\mathbf{hebb}_{\boldsymbol{\mu}}$**(..)** and $\mathbf{scm}_{\boldsymbol{\alpha}}$**(..)** and combination function weights $\boldsymbol{\gamma_1}$ and $\boldsymbol{\gamma_2}$ provides:

$$\begin{aligned} X_{11} &= \boldsymbol{\gamma_1}\mathbf{hebb}_{\boldsymbol{\mu}}(X_1, X_6, X_{11}) + \boldsymbol{\gamma_2}\mathbf{scm}_{\boldsymbol{\alpha}}(X_1, X_6, X_{11}, -0.7\,X_{10}) \\ X_{12} &= \boldsymbol{\gamma_1}\mathbf{hebb}_{\boldsymbol{\mu}}(X_1, X_7, X_{12}) + \boldsymbol{\gamma_2}\mathbf{scm}_{\boldsymbol{\alpha}}(X_1, X_7, X_{12}, -0.7\,X_{10}) \end{aligned}$$

$$\begin{aligned} X_{11} &= \boldsymbol{\gamma_1}(X_1X_6(1 - X_{11}) + \boldsymbol{\mu}\,X_{11}) + \boldsymbol{\gamma_2}(X_{11} - 0.7\,\boldsymbol{\alpha}\,X_{11}(1 - X_{11})X_{10}) \\ X_{12} &= \boldsymbol{\gamma_1}(X_1X_7(1 - X_{12}) + \boldsymbol{\mu}\,X_{12}) + \boldsymbol{\gamma_2}(X_{12} - 0.7\,\boldsymbol{\alpha}\,X_{12}(1 - X_{12})X_{10}) \end{aligned}$$

However, these equations are not linear and more difficult to be solved algebraically. Nevertheless, they still can be used for verification by substitution of values found in simulations. The values used are

$$\boldsymbol{\gamma_1} = 0.85 \quad \boldsymbol{\gamma_2} = 0.15 \quad \boldsymbol{\mu} = 0.8 \quad \boldsymbol{\alpha} = 0.5 \quad X_1 = A_1 = 1$$

Then the instantiated equations are

$$\begin{aligned} X_{11} &= 0.85(X_6(1 - X_{11}) + 0.8X_{11}) + 0.15(X_{11} - 0.35\,X_{11}(1 - X_{11})X_{10}) \\ X_{12} &= 0.85(X_7(1 - X_{12}) + 0.8X_{12}) + 0.15(X_{12} - 0.35\,X_{12}(1 - X_{12})X_{10}) \end{aligned}$$

The relevant equilibrium values obtained in the simulation are

$$\begin{aligned} X_6 &= 0.217599600251934 \quad & X_{11} &= 0.502555992556694 \\ X_7 &= 0.602153273449135 \quad & X_{12} &= 0.742898464938841 \\ X_{10} &= 0.526788924575543 \end{aligned}$$

After substitution of these in the instantiated equations, the following is obtained:

$$0.502214624461369 = 0.502555992556694$$
$$0.742915691976951 = 0.742898464938841$$

The deviations of these equations are −0.0003413680953248120 and 0.0001722703810991 27 respectively, which both are less than 0.001. This provides evidence that also for the reification states used for adaptation of the connections the model does what is expected.

5.7 Discussion

In this chapter, a second-order adaptive reified temporal-causal network model was presented for the adaptive role of stress in decision making based on the disconnect-reconnect principle (Sousa and Almeida 2012). Parts of this chapter are based on Treur and Mohammadi Ziabari (2018). In this computational network model, connections developed in the past are suppressed due to acute stress as a form of reset (disconnect) and Hebbian learning takes place to adapt the decision making to the stressful conditions (reconnect). A number of simulations were performed two of which were presented in the chapter. Findings from Neuroscience were taken into account in the design of the adaptive model (Quaedflieg et al. 2015; Hermans et al. 2014; Reser 2016; Sousa and Almeida 2012). This literature reports experiments and measurements for stress-induced conditions as addressed from a computational perspective in the current chapter. In addition to this, also metaplasticity has been incorporated in the adaptive network model. This makes it a second-order adaptive network model. In the simulations, it has been shown how this second-order adaptation accelerates the learning effect, on top of the disconnect-reconnect principle, as also claimed in another context by Robinson et al. (2016). Also, a precise mathematical analysis has been done to verify that behaviour of the reified network model is as expected.

In other, more applied literature, such as Gok and Atsan (2016), not the Neuroscience perspective is followed, but a more general psychological perspective on decision making applied to a manager's context. This may seem to contrast with the Neuroscience perspective followed in the current chapter which is mainly based on Sousa and Almeida (2012). However, the more refined approach on decision making and its subprocesses in Gok and Atsan (2016), such as the generation of decision options and selection of an option, may provide interesting inspiration for future research in making a more refined version of the current model, and place it in a more applied context. Another future extension may address an explicit role for cortisol in the development of stress. The current states used to model the extreme emotion (ps_{ee} and fs_{ee}) can be seen as aggregate states for a number of brain states, including the cortisol level. In a more refined approach different substates may be distinguished, under which a separate state for the cortisol level.

This network model can be used as the basis of a virtual agent model to get insight in such processes and to consider certain support or treatment of individuals to handle extreme emotions when they have to work in a stressful context condition and prevent some stress-related disorders that otherwise might develop. In future research, other scenarios will be addressed and simulated for individuals with different characteristics.

References

Barsegyan, A., Mackenzie, S.M., Kurose, B.D., McGaugh, J.L., Roozendaal, B.: Glucocorticoids in the prefrontal cortex enhance memory consolidation and impair working memory by a common neural mechanism. Proc. Natl. Acad. Sci. USA **107**, 16655–16660 (2010)

de Kloet, E.R., Joëls, M., Holsboer, F.: Stress and the brain: from adaptation to disease. Nat. Rev. Neurosci. **6**, 463–475 (2005)

Etkin, A., Prater, K.E., Hoeft, F., Menon, V., Schatzberg, A.F.: Failure of anterior cingulate activation and connectivity with amygdala during implicit regulation of emotional processing in generalized anxiety disorder. Am. J. Psychiatry **167**, 545–554 (2010). https://doi.org/10.1176/ajp.2009.09070931 PMID: 201123913

Glass, D.C., Reim, B., Singer, J.E.: Behavioral consequences of adaptation to controllable and uncontrollable noise. J. Exp.Soc. Psychol. **7**, 244–257 (1971)

Gok, K., Atsan, N.: Decision-making under stress and its implications for managerial decision-making: a review of literature. Int. J. Bus. Soc. Res. **6**(3), 38–47 (2016)

Hermans, E.J., Hencknes, M.J.A.G., Joels, M.: Guillen Fernandes: dynamic adaption of large-scale brain networks in response to acute stressors, Trends Neurosci. **37**(6), 304–14 (2014). https://doi.org/10.1016/j.tins.2014.03.006. Epub

Johnstone, T., van Reekum, C.M., Ury, H.L., Klain, N.H., Davidson, R.J.: Failure to regulate: counterproductive recruitment of top-down prefrontal-subcortical circuitry in major depression. J. Neurosci. **27**, 8877–8884 (2007). PMID: 17699669

Quaedflieg, C.W.E.M., van de Ven, V., Meyer, T., Siep, N., Merckelbach, H., Smeets, T.: Temporal dynamics of stress-induced alternations of intrinsic amygdala connectivity and neuroendocrine levels. PLoS ONE **10**(5), e0124141 (2015). https://doi.org/10.1371/journal.pone.0124141

Radley, J., Morrison, J.: Repeated stress and structural plasticity in the brain. Ageing Res. Rev. **4**, 271–287 (2005)

Reser, J.E.: Chronic stress, cortical plasticity and neuroecology. Behave Process. (2016). https://doi.org/10.1016/j.beproc.2016.06.010. Epub

Robinson, B.L., Harper, N.S., McAlpine, D.: Meta-adaptation in the auditory midbrain under cortical influence. Nat. Commun. **7**, 13442 (2016)

Sousa, N., Almeida, O.F.X.: Disconnection and reconnection: the morphological basis of (mal) adaptation to stress. Trends in Neurosci. **35**(12), 742–51 (2012). https://doi.org/10.1016/j.tins.2012.08.006. Epub 2012 Sep 21

Treur, J.: Verification of temporal-causal network models by mathematical analysis. Vietnam J. Comput. Sci. **3**, 207–221 (2016a)

Treur, J.: Network-Oriented Modeling: Addressing Complexity of Cognitive, Affective and Social Interactions. Springer Publishers, Berlin (2016b)

Treur, J.: Network reification as a unified approach to represent network adaptation principles within a network. In: Proceedings of the 7th International Conference on Natural Computing. Lecture Notes in Computer Science, vol. 11324, pp. 344–358. Springer Publishers, Berlin (2018a)

Treur, J.: Multilevel network reification: representing higher order adaptivity in a network. In: Proceedings of the 7th International Conference on Complex Networks and their Applications, ComplexNetworks'18, vol. 1. Studies in Computational Intelligence, vol. 812, pp. 635–651, Springer Publishers, Berlin (2018b)

Treur, J., Mohammadi Ziabari, S.S.: An adaptive temporal-causal network model for decision making under acute stress. In: Nguyen, N.T., Trawinski, B., Pimenidis, E., Khan, Z. (eds.) Computational Collective Intelligence: Proceedings of the 10th International Conference, ICCCI'18, vol. 2. Lecture Notes in Computer Science, vol. 11056, pp. 13–25. Springer Publishers, Berlin (2018)